Microfluidic platform for the real time measurement and observation of endothelial barrier function under shear stress

Daniel M. Lewis,[1,2,a)] Nicholas Mavrogiannis,[1,a)] Zachary Gagnon,[1] and Sharon Gerecht[1,2,3,b)]
[1]*Department of Chemical and Biomolecular Engineering, Johns Hopkins University, Baltimore, Maryland 21218, USA*
[2]*Johns Hopkins Physical Sciences–Oncology Center and Institute for NanoBioTechnology, Johns Hopkins University, Baltimore, Maryland 21218, USA*
[3]*Department of Materials Science and Engineering, Johns Hopkins University, Baltimore, Maryland 21218, USA*

(Received 25 February 2018; accepted 10 April 2018; published online 15 May 2018)

Electric cell-substrate impedance sensing (ECIS) is a quickly advancing field to measure the barrier function of endothelial cells. Most ECIS systems that are commercially available use gold electrodes, which are opaque and do not allow for real-time imaging of cellular responses. In addition, most ECIS systems have a traditional tissue culture Petri-dish set up. This conventional set-up does not allow the introduction of physiologically relevant shear stress, which is crucial for the endothelial cell barrier function. Here, we created a new ECIS micro-bioreactor (MBR) that incorporates a clear electrode made of indium tin oxide in a microfluidic device. Using this device, we demonstrate the ability to monitor the barrier function along culture of cells under varying flow rates. We show that while two cell types align in the direction of flow in responses to high shear stress, they differ in the barrier function. Additionally, we observe a change in the barrier function in response to chemical perturbation. Following exposure to EDTA that disrupts cell-to-cell junctions, we could not observe distinct morphological changes but measured a loss of impedance that could be recovered with EDTA washout. High magnification imaging further demonstrates the loss and recovery of the barrier structure. Overall, we establish an ECIS MBR capable of real-time monitoring of the barrier function and cell morphology under shear stress and allowing high-resolution analysis of the barrier structure. *Published by AIP Publishing*. https://doi.org/10.1063/1.5026901

INTRODUCTION

The cell barrier is very important for controlling diffusion in organs. Cells form this barrier by forming tight junctions with neighboring cells. This applies very specifically to endothelial cells (ECs) that line the inner of blood vessels to control transport of essential nutrients to most of the body's organs.[1–3] The EC barrier function is critical for a variety of physiological pathways such as the control of transport of small molecules through the blood brain barrier[4] and kidney function.[5] The EC barrier function is also crucial in understanding the intricacies of cancer such as extravasation,[6] intravasation,[7] and response to chemotherapeutics.[8] Current technology to understand the barrier function is monitored via trans-epithelial/trans-endothelial electrical resistance (TEER) or electric cell-substrate impedance sensing (ECIS). In TEER systems, a direct current is used, while in the ECIS based system, an alternating current (AC) is used. The

[a)]D. M. Lewis and N. Mavrogiannis contributed equally to this work.
[b)]Author to whom correspondence should be addressed: gerecht@jhu.edu. Tel.: +1-410-516-2846. Fax: +1-410-516-5510.

benefit of alternating current is that it reduces cell death from the electrical current.[9] In both systems, gold electrodes are used as well a chamber cell system to analyze the barrier. Using these systems, it is impossible to image morphological changes of cells in real time due to the opacity of the culture compartment. Moreover, it would be desirable to add physiological/mechanical cues, such as shear stress, which are critical to the function of the EC barrier.

Due to the toxicity risks associated with TEER, there has been a rise in the use of ECIS. ECIS is a sensitive, label-free technique for characterizing and monitoring cells *in vitro*. Using ECIS, it is possible to monitor an array of cell activities including morphological changes,[10] cell motility,[11] as well as other behaviors directed by the cytoskeleton;[12] however, due to the large gold electrodes, live-cell monitoring cannot be performed. ECIS operates by monitoring the impedance between sensing and working electrodes. Traditionally, thin gold electrodes are deposited onto the surface of a cell-culture dish. The system works by measuring impedance changes with a weak, non-invasive alternating current (AC) electric field. The AC impedance of the cell-covered electrode is then measured at one or several frequencies as a function of time. Due to the insulating properties of their membranes, the cells behave like dielectric particles so that the impedance increases with increasing coverage of the electrode until a confluent (i.e., continuous) layer of cells is established. In the confluent cell layer, the measured impedance is mainly determined by the three-dimensional shape of the cells. If cell shape changes occur, the current pathways through and around the cell bodies change as well, leading to a corresponding increase or decrease in impedance. Thus, by recording time-resolved impedance measurements, cell shape changes can be followed in real time with sub-microscopic resolution and can be used for bio-analytic purposes.

In ECIS, electrode parameters are crucial to accurately monitor sensitive changes in the cell function. Typically, large working electrodes are used when cell density is sparse, such as cell proliferation studies. Larger electrodes or a large array of smaller electrodes decrease the variability of measurements. When studying the barrier function, cell membrane capacitance, as well as the spacing between the cell basal membrane and the electrode, smaller electrodes are typically used. When using smaller electrodes, the sensing electrode is generally on the size order of 10^3 cm or smaller since a resistance component from a bulk electrolyte (normally cell culture medium) dominates the measured impedance when a larger electrode is used. The main benefit of using smaller electrode arrays is the ability to study sub-micron morphological changes in cells due to stimuli. The standard material for electrodes is gold, typically a chrome-gold, or titanium-gold layer. Gold is a highly conductive material with little to no variation in fabrication as well as being cell-compatible. One significant drawback when using gold is that the electrodes are opaque, eliminating the use of standard microscopy. As a means to alleviate this set back, we have fabricated co-planar electrodes using indium tin oxide (ITO).

Indium tin oxide (ITO) is a conductive metal which, when treated, becomes transparent; it is also a cell-compatible metal. While this is not the first demonstration of ECIS using impedance spectroscopy,[13–16] it has not been frequently used in the past two decades. ITO is generally overlooked for a few significant reasons: lower conductivity and variability between fabrications and being generally more difficult to manage. Another set back, which also leads to increased variability, is the process by which the metal is made transparent. While making electrodes more transparent is better for imaging purposes, the relationship between transparency and conductivity is inversely proportional. Therefore, when electrodes become more transparent, the conductivity decreases, limiting the sensitivity of the electrodes.

In this study, we sought to establish a new ECIS system combining microfluidics with impedance sensing. Previous studies have incorporated microfluidics with ITO electrodes but have examined the effect of using a microfluidic device under gravity driven flow.[15,16] Here, we test cellular responses in higher shear regimes, which are physiologically relevant shear stresses. Taking advantage of the ITO, we were able to visualize how the cell morphology changes in response to various stimuli while measuring impedance. We present coplanar ITO electrodes capable of sensitively monitoring barrier functions of EC cells subjected to different stimuli, namely, shear stress and biochemical supplementation.

MATERIALS AND METHODS

Device fabrication

A single microfluidic channel device was fabricated using standard soft photolithography and microfabrication techniques. First, microchannel electrodes were fabricated using a lift-off process. Glass cover slips (50 × 30 mm, no.1, Fisher Scientific) were patterned with a sacrificial layer of a positive photoresist (Shipley 1813), and 180 nm of ITO was deposited onto the patterned coverslips. The coverslips were then exposed to acetone to the sacrificial layer, leaving the desired electrode pattern. Since ITO is not solder compatible, another layer of metal was deposited onto the coverslips. The electrode patterned was covered, and a 10:30 nm layer of chromium:gold was deposited onto the electrode pads where wire leads could be soldered. The microchannel was fabricated in Polydimethylsiloxane (PDMS) (Momentive, RTV 615A). A 10:1 mixture of PDMS elastomer and curing agent was poured atop the wafer and baked at 85 °C for 50 min. The PDMS was gently peeled off the wafer and fluid ports were punched with a 0.75 mm diameter biopsy punch (Ted Pella, Inc.). The PDMS microchannel and electrode pattern were then exposed to oxygen plasma (Jelight, Model 42A) and immediately aligned and sealed under an inverted microscope. The device consists of a main flow channel of 250 μM width and 250 μM height. The embedded electrodes consist of circular pads with a radius of 50 μm. To ensure that there was no cross-talk between electrodes, each pad was separated by 150 μm, which was verified with COMSOL simulations.

COMSOL simulation

Simulations were performed to ensure that there was no cross-talk among electrodes. Cross talk eliminates the sensitivity of the electrodes, thereby limiting the ability to sense morphological changes of the cells, specifically their barrier functions. The ac electric field path and magnitude were simulated for three electrode pads. An autocad file was imported into COMSOL (COMSOL Multiphysics) with the exact specifications of the electrode array, with the exception of shortening the length. In addition, flow simulation was used to model the shear stress in the channel as previously reported.[17]

Cells

Human umbilical vein endothelial cells (HUVECs) were cultured using endothelial cell growth medium (EGM: PromoCell, Heidelberg, Germany). The HUVECs (passages 3–6; PromoCell) were passaged every 3 to 4 days in 0.05% trypsin. The human neonatal foreskin fibroblast (NuFF) cell line was obtained from Global Stem (Rockville, MD; #GSC-3002) at passage 9. NuFF cells were cultured in Dulbecco's Modified Eagle's medium (DMEM) supplemented with 10% vol/vol heat inactivated FBS (Life Technologies).

Microbioreactor seeding

Microbioreactor (MBR) preparation was performed as previously described.[8,17] The device was exposed to ultra-violet light for 15 min and then cleared with 3 ml of 100% ethanol followed by 3 ml of phosphate-buffered saline (PBS). 50 μg/ml of fibronectin (Fn), for HUVECs, or 50 μg/ml of collagen, for NuFFs, were flown into the device and allowed to incubate at room temperature overnight. The channel was then rinsed with the cells' respective media prior to seeding. Prior to seeding, baseline impendence measurements were taken. HUVECs and NuFFs were added into the MBR at a density of 6×10^6 cells per ml by injecting them through the media inlet port. The cells were left attached at 37 °C for 3 h. 3 h was chosen based on the calculations in the study by Abaci *et al.*[18] In short, the channel height and width as well as the time allowed for detached are chosen based on the cell consumption rate of glucose in the media. In high shear and physiological condition experiments, media was circulated at a flow rate of 14 ml/h between the microbioreactor and a media reservoir using a peristaltic pump

(Ismatec, Wertheim, Germany). For low shear experiments, the same pump was used and flown at a rate of 1.18 ml/h.

ECIS measurements

An impedance spectrometer (Agilent 4192A) was connected to the electrode array and used to measure the magnitude of the impedance under varying external conditions. For all impedance measurements, a sine-modulated AC potential of 50 mV was applied to the electrode array and the magnitude and phase angle of impedance were measured over an excitation frequency range between 5 and 50 kHz. This range was chosen as any frequency lower than 5000 Hz was purely resistive, and for higher than 50 kHz, more current capacitively couples directly through the insulating cell membrane. A labview script was coded to actuate the impedance spectrometer every 15 min to perform a frequency sweep over the specified range. The data were saved and uploaded to a MATLAB script for post processing.

Since ITO fabrication is not consistent from batch to batch, the data obtained were normalized as to compare each trial. A baseline measurement was performed prior to cell loading where the impedance of the electrode/media system was measured across the specific frequency range. Furthermore, baseline measurements with confluent cells were performed prior to stimulating the cells in the experiments. All data were normalized to these baseline measurements to eliminate any variation due to the electrodes, cell media, or cells themselves.

EDTA experiments

Cells were exposed to low shear (1.18 ml/h) using a syringe pump with complete HUVEC media (Chemyx, Stafford, TX). The media was then replaced with complete HUVEC media supplement with 2 mM EDTA and flown in for 30 min. The cell solution was switched again to complete HUVEC media, and the cells were allowed to rebound. This was repeated multiple times.

Data analysis

Matlab (MathWorks, Inc.) scripts were written to process the frequency sweep taken at each time point. First, the background impedance was calculated prior to seeding by taking three frequency sweeps. The impedance value is dependent upon frequency used to take the reading.[19] The optimal frequency was determined by finding the largest difference in the resistance of the electrode with and without cells at a given frequency. This allows for chip to chip variation to be normalized. This can also be done by plotting the resistance of the cell covered electrode divided by the resistance of the cell free electrode versus time. The peak of this graph will be the ideal frequency for the system.[20] Once the ideal frequency was determined, the real impedance was then calculated over different chemical and physiological conditions.

Immunofluorescent staining and imaging

We analyzed the cellular morphology and protein localization using fluorescent imaging of fixed cells as shown previously.[8] All solutions used for fixation and staining were injected into the MBR at a flow rate of 1 ml/h for a volume of 300 μl. Cells were fixed using 3.7% paraformaldehyde solution for 15 min at room temperature, permeabilized with 0.1% Triton X-100 for 15 min, and then stained with VECAD (1:200 Santa Cruz Biotechnology, Santa Cruze, CA), Phalloidin (1:1000), and 4=6-diamidino-2-phenylindole (DAPI) (1:1000). After each solution, the MBR was rinsed with PBS, and for immunofluorescent labeling, cells were incubated overnight with anti-mouse VECAD (1:500; ThermoFisher). The fluorescently labeled MBR was examined using confocal microscopy (LSM 780; Carl Zeiss).

Statistics

All experiments were performed on triplicate samples. Graphs were plotted using standard deviation (SD). Significance levels were determined using unpaired two-tailed t-tests where appropriate (GraphPad Prism) and set at $*P < 0.05$, $**P < 0.01$, and $***P < 0.005$.

RESULTS AND DISCUSSION

Electrode design and model

A single microfluidic channel device was designed to incorporate the electrode components (ITO) within a cell culture channel [Fig. 1(a)]. The electrode was placed in the center portion of the channel and in the middle between the inlet and outlet ports. Traditionally with ECIS systems, the electrodes are placed on the substrate side of the cell monolayer. Alternative ECIS measurements have the electrodes placed on either side of the cell, but the electrode placement can vary drastically from trial to trial complicating measurements and leading to inconsistencies. In the ECIS MBR, the electrodes are placed on the substrate side of the cell, allowing reproducibility. This design was further chosen to minimize the amount of frequency needed to monitor cell response, due to the current passing directly through the cells and not being obstructed by the bulk media. These lower frequencies also allow for greater sensitivity since the frequency is only passing through the cells. In order to fabricate the ITO electrodes, ITO was first deposited on glass coverslips and then annealed to make optically clear, and finally, gold was deposited onto the pads to allow for soldering of wires. This allowed us to establish a fixed contact between the chip and the wires [Fig. 1(b)]. The electrode geometry consisted of active circular pads surrounded by reference electrodes. The pads were designed to be small, $\sim$50 μm, to ensure that current passes through the entire cell monolayer. Also, fabricating smaller electrodes is optimal for monitoring barrier functions of the cells. A COMSOL simulation was performed to fully define the path of the electric field. The pads sat 150 μm apart, attached by 10 μm wide connectors. The COMSOL simulation [Fig. 1(c)] illustrates the electric potential distribution produced by the electrode geometry. A simulation of an electric potential

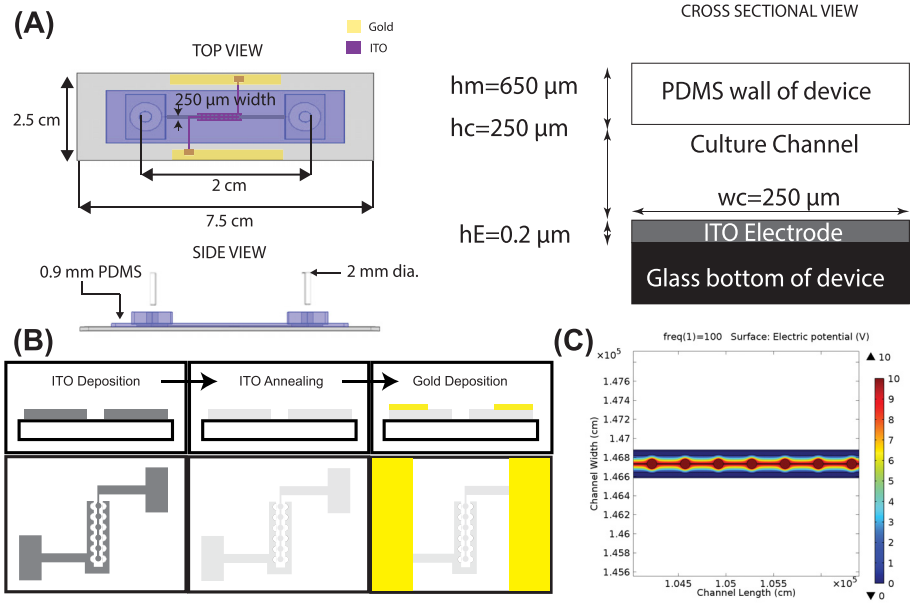

FIG. 1. ECIS Model: (a) Schematic of the ECIS MBR is shown in top, down, and side views. hE is the height of the ITO electrode, hc is the height of the tissue culture channel, wc is the width of the tissue culture channel, and hm is the height of the PDMS wall of the device. (b) Microfabrication process to create the electrode array. ITO is deposited to create a specific pattern. The ITO is then treated and annealed to create a transparent electrode. Finally, a layer of gold is deposited onto the pads. (c) COMSOL simulations were performed to study the electric potential of the ITO electrode design.

at 10 V was applied to the circular pads, and the surrounding electrode structures were held at ground. Based on the potential distribution in Fig. 1(c), the electric field travels down the potential gradient from the circular pads to the reference electrode array, with a maximum field strength on the circular pads. We found that this separation distance, regions of high electric potential, increased in the vicinity of the circular electrodes and resulted in increased device sensitivity. The size of the circular pads and this resulting sensitivity can be modified depending on the experimental design.

ECIS MBR design, fabrication, and cell culture

The ECIS MBR was designed similar to our previously studies.[8,17,18] A previously developed bubble trap was added to prevent bubbles from shearing cells off the channel[8] [Fig. 2(a)]. A square channel was used due to the simplicity of the fabrication, which allows for equal distribution and coverage of various cell types [Fig. 2(b)]. The rectangular shape minimizes non-uniform shear stress as previously reported.[17] Additionally, COMSOL simulations were performed to analyze the shear profile of the channels at 1 and 12 dynes/cm^2. The non-uniform shear stress is limited to a distance of 50 μm from the wall towards the center of the channel (Supplementary Fig. 1). PDMS was used as the material for the channel due to its high gas permeability and the ability for it to do precise replica molding. This set up allows us to create a channel to mimic fluid shear stress similar to physiological levels. Cells are seeded onto the channel and allowed to attach for 3 h, and then, media is immediately perfused through the channel at the desired flow rate [Figs. 2(c) and 2(d)]. For longer experiments, the bioreactor was connected to a peristaltic pump to allow for continuous media perfusion at a higher flow rate. This allows for chip-to-chip variation to be normalized. At specific time points, the measured impedance over the applied frequency range was compared. The script isolated the impedance measurements for the specific excitation frequency, which was used to monitor cells subjected to external stimuli and how their barrier functions were affected.

Live monitoring of the barrier function in HUVEC and NuFF

To take advantage of the transparent ITO and the microfluidic aspect of the chip, we used HUVECs and NuFFs. HUVECs were chosen for their ability to form a barrier, while NuFFs were chosen due to their lack of the barrier. In order to ensure attachment, the ECIS MBR

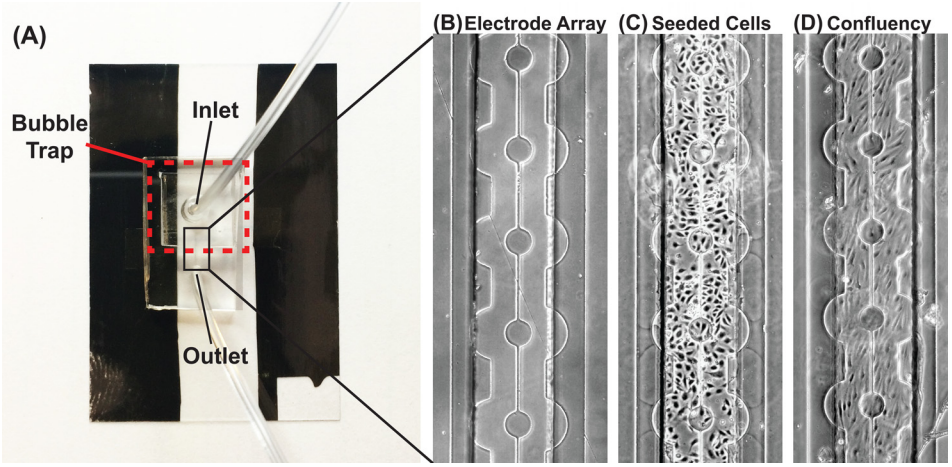

FIG. 2. The ECIS MBR: (a) Image of the microfluidic device with the embedded electrode array. A bubble trap is fabricated at the inlet port. Gold pads are fabricated onto the ITO pads to allow for soldering, whereby the impedance spectrometer is connected. (b) 2D micrograph of the electrode array. ITO circular pads are connected and centered within the microfluidic device. The counter electrode surrounds the circular pads. (c) Micrograph of HUVEC cells seeded into the microfluidic device. (d) Micrograph of a confluent layer of HUVEC cells on the electrode array after 24 h. Scale bar: 100 μm.

channel was coated with fibronectin (for HUVECs) to the ITO, while collagen was used to adhere NuFFs to the ITO. In order to account for the different medias and extracellular matrix coatings, a frequency sweep was performed from 500 to 30 000 Hz after coating and with the relevant cell media. This allowed us to subtract off the background signal regardless of whether media and protein coating were in contact with the ITO.

Following cell seeding, the barrier function in response to low (1 dynes/cm^2) and high (12 dynes/cm^2) shear stresses was analyzed. Monitoring the differences in impedance between the cells subjected to normal shear versus high shear allowed us to determine the optimal excitation frequency. We chose a frequency of 5000 Hz as the optimal frequency as it yielded the starkest difference. HUVECs align in the direction of the flow when exposed to high shear stress for 24 h [Fig. 3(a)], in agreement with well established data.[8,18,21–23] Interestingly, NuFFs exhibited similar responses with their directional alignment when exposed to high shear stress [Fig. 3(b)]. We noticed that the NuFF morphology is more spindle like and elongated compared with HUVECs cultured under the same conditions. NuFFs are also found to be less contact inhibited and seem to not become quiescent under shear. This is the first time this phenomenon has been observed.

Next, we measured the resistance over the monolayer along the culture period. Figure 3(c) shows a representative impedance reading during the culture period. We noticed that when flow is introduced, an immediate increase in resistance of HUVECs is reported, while NuFF resistance does not change. At low shear stress, we observed that HUVECs have a significantly higher resistance compared to NuFFs [Fig. 3(d)]. HUVECs have 20% higher resistance values compared to NuFFs at low shear. At the moment in which both cell types were exposed to high shear stress, we observed a greater change in resistance in HUVECs, while there is no change in resistance in the NuFF monolayer (Supplementary Fig. 2). Additionally, HUVECs had a significantly higher resistance, 60% higher, compared to NuFFs when they were maintained at high shear [Fig. 3(e)], demonstrating how higher shear stress improves the barrier function of vein endothelial compared to NuFFs. In order to take advantage of the ITO, we measured cell alignment at 1 and 12 dynes/cm^2, where an alignment of 0 degrees is aligned with the direction of flow. At 1 dynes/cm^2, HUVECs and NuFFs had a similar alignment in response to flow [Fig. 3(f)]. At 12 dynes/cm^2, both cells aligned with the flow. Additionally, the cell aspect ratio, ratio of the major to minor axes, was calculated at 1 and 12 dynes/cm^2, where an aspect ratio of 1 is a round cell. At 1 dynes/cm^2, HUVECs and NuFFs had a very similar aspect ratio, while at 12 dynes/cm^2, NuFFs elongate more under shear stress, compared to HUVECs. Overall, taking full advantage of the ITO, we were able to simultaneously monitor the morphological and barrier changes on the electrodes. These results demonstrate the advantage of the ECIS MBR

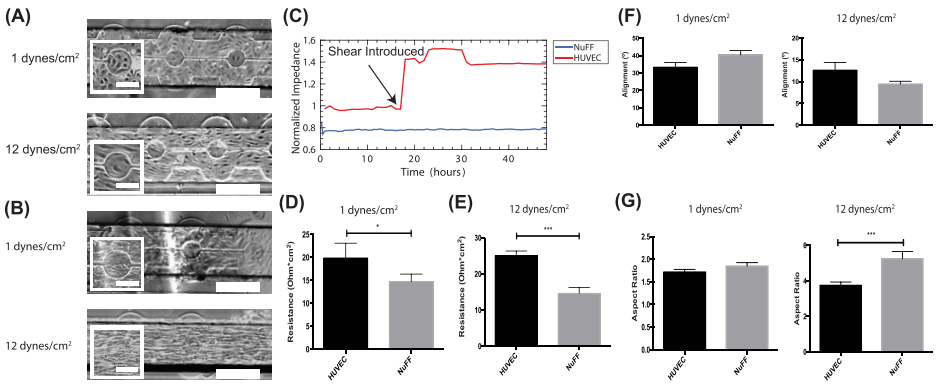

FIG. 3. HUVEC and NuFF response to shear stress: Representative bright-field images of HUVECs (a) and NuFFs (b) seeded in the MBR treated with 1 or 12 dynes/cm^2. (c) A representative impedance reading along the culture period. The resistance value at each shear stress was averaged over all trials and shows that HUVECs have a higher barrier function than NuFFs at 1 dynes/cm^2 (d) and 12 dynes/cm^2 (e). Scale bars are 50 μm and 200 μm. (f) Alignment of the cells in the microfluidic devices at 1 and 12 dynes/cm^2. (g) Aspect ratio of the cells in the microfluidic device at 1 and 12 dynes/cm^2.

demonstrating the barrier function difference when cells exhibit a similar morphological response to shear stress.

HUVEC barrier disruption

To evaluate the sensitivity of the ITO metal, we next tested a well understood chemical response. In order to break down cadherin junctions in cells, EDTA is commonly used as a calcium chelator.[24] In our ECIS MBR, we measured the effect of flowing 2 mM EDTA on the barrier structure of HUVECs at 1 dyne/cm^2. We could not detect morphological changes when using brightfield microscopy [Fig. 4(a)]. We next used confocal microscopy to examine immunofluorescence stain of VE-cadherin (vascular endothelial cadherin) as a marker for barrier integrity. We found that after EDTA treatment, a reduction in VECAD is observed, which is restored after washing out with complete HUVEC media [Fig. 4(b)]. However, measuring impendence, we observed a $7.96 \pm 0.3\%$ decrease in the endothelial barrier function after EDTA treatment. We further examined the loss and recovery of the HUVEC barrier function. We found that washing with media without EDTA allowed for the HUVEC barrier to fully recover [Fig. 4(c)]. Overall, the transparency of the ECIS MBR allows us to use both brightfield and confocal microscopy techniques for low and high resolution analyses of the barrier response while correlating those with resistance measurements.

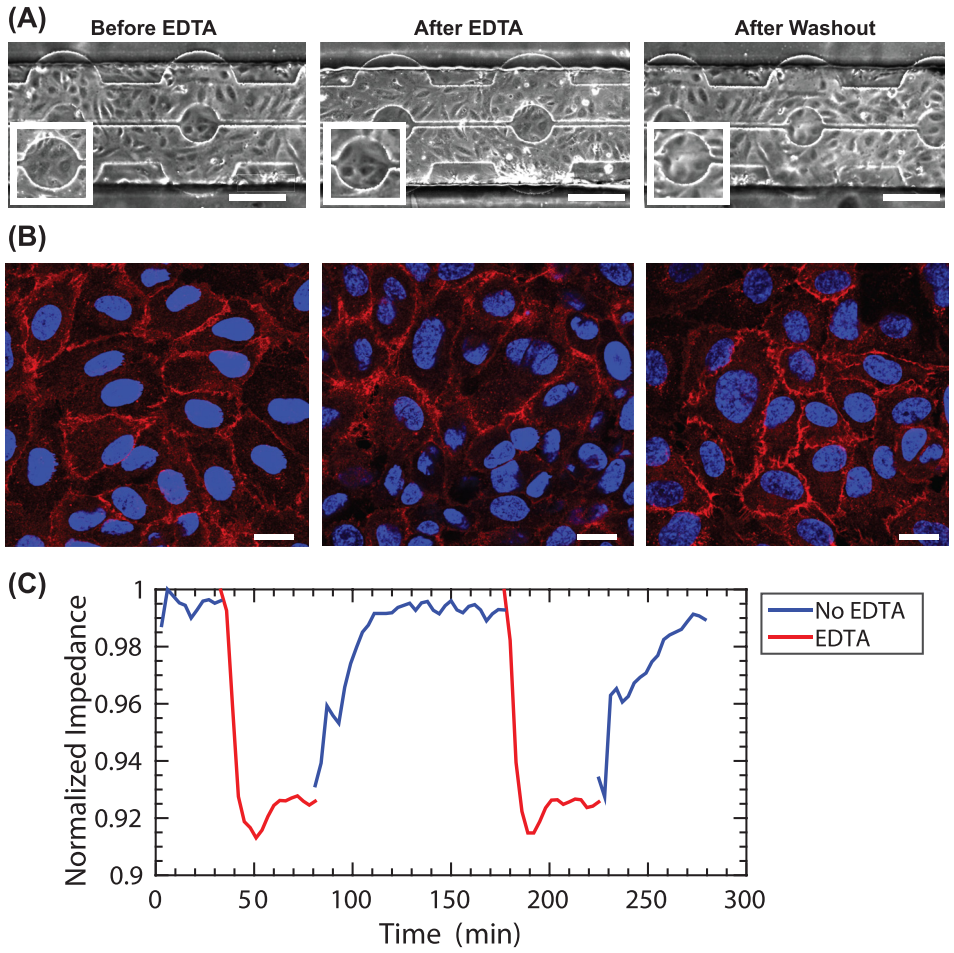

FIG. 4. Impact of EDTA Treatment on the barrier: (a) Brightfield and (b) confocal microscopy of HUVECs treated before EDTA treatment, during 2 mM EDTA treatment, and after they are recovered with normal media, scale bar: 200 μm. HUVECs were also stained for VECAD (red) and DAPI (blue), scale bar: 20 μm. (c) A representative impedance reading along the culture period is shown during the treatment and recovery phases of HUVECs treated with 2 mM EDTA at 1 dyne/cm^2.

CONCLUSION

We established ECIS MBR enabling us to quantitatively analyze the cell barrier, while simultaneously observing the cell morphology under physical or chemical cues. We demonstrate the two capabilities: one where morphological monitoring of the cells is impacted by physical cue and the other where chemical cue is introduced, inducing a quantitative change in impedance without the change in the cell morphology. From the first case, we were able to show that under higher shear, NuFFs align with the direction of the flow, similar to HUVECs. Here, the HUVEC barrier function increases with shear stress, while the NuFF barrier remains constant even with a change in the cell morphology. Second, with EDTA supplementing experiments, we were able to show how chemical interference disturbs the barrier function without observable changes in the cell morphology and that the barrier function can be quickly restored once the EDTA is washed out. Here, we further leveraged the optically clear electrodes to analyze the barrier structure using high-resolution confocal microscopy. These experiments demonstrate the applicability of the ECIS MBR, allowing the analysis of cellular responses to physiologically relevant shear stress and dynamic chemical perturbation while live monitoring of cell morphology and impendence. In the future, this chip can be utilized to examine a variety of applications from cancer cell extravasation under shear, vascular side-effects to different therapeutics, such as fluorouracil, or even as a system to study the effects of shear on the blood brain barrier in a physiologically relevant flow regime. Furthermore, ITO electrodes can be applied to traditional ECIS experiments in which the cells sit atop a semi-permeable membrane and are monitored via impedance.

SUPPLEMENTARY MATERIAL

See supplementary materials for figures showing COMSOL Simulation of shear stress in the channel and percent change in resistance in response to shear stress in HUVECs and NUFF.

ACKNOWLEDGMENTS

We thank Quinton Smith for his technical assistance with setting up the microfluidic device. This work was supported by a fellowship from the NCI T-32 2T32CA153952–06 and a Nanotechnology Cancer Research training Grant (to D.M.L.) and 15EIA22530000 from American Heart Association and U54CA210173 from the NCI Physical Sciences-Oncology Center (both to S.G.).

[1]C.-W. Cho, Y. Liu, W. N. Cobb, T. K. Henthorn, K. Lillehei, U. Christians, and K.-Y. Ng, Pharm. Res. **19**(8), 1123–1129 (2002).
[2]W. Zhou, M. Y. Fong, Y. Min, G. Somlo, L. Liu, M. R. Palomares, Y. Yu, A. Chow, S. T. F. O'Connor, and A. R. Chin, Cancer Cell **25**(4), 501–515 (2014).
[3]S. F. Rodrigues and D. N. Granger, Tissue Barriers **3**(1-2), e978720 (2015).
[4]M. Gumbleton and K. L. Audus, J. Pharm. Sci. **90**(11), 1681–1698 (2001).
[5]J. Malyszko, Clin. Chim. Acta **411**(19), 1412–1420 (2010).
[6]S. Weis, J. Cui, L. Barnes, and D. Cheresh, J. Cell Biol. **167**(2), 223–229 (2004).
[7]I. K. Zervantonakis, S. K. Hughes-Alford, J. L. Charest, J. S. Condeelis, F. B. Gertler, and R. D. Kamm, Proc. Natl. Acad. Sci. **109**(34), 13515–13520 (2012).
[8]H. E. Abaci, Y.-I. Shen, S. Tan, and S. Gerecht, Sci. Rep. **4**, 4951 (2014).
[9]K. Benson, S. Cramer, and H.-J. Galla, Fluids Barriers CNS **10**(1), 5 (2013).
[10]P. O. Bagnaninchi and N. Drummond, Proc. Natl. Acad. Sci. **108**(16), 6462–6467 (2011).
[11]J. Hong, K. Kandasamy, M. Marimuthu, C. S. Choi, and S. Kim, Analyst **136**(2), 237–245 (2011).
[12]N. S. Umapathy, E. A. Zemskov, J. Gonzales, B. A. Gorshkov, S. Sridhar, T. Chakraborty, R. Lucas, and A. D. Verin, J. Cell. Physiol. **223**(1), 215–223 (2010).
[13]L. Yang, C. Hsu, and Y. Ou, Paper presented at 16th International the Solid-State Sensors, Actuators and Microsystems Conference (TRANSDUCERS) (2011).
[14]C. Tlili, K. Reybier, A. Géloën, L. Ponsonnet, C. Martelet, H. B. Ouada, M. Lagarde, and N. Jaffrezic-Renault, Anal. Chem. **75**(14), 3340–3344 (2003).
[15]T. A. Nguyen, T.-I. Yin, D. Reyes, and G. A. Urban, Anal. Chem. **85**(22), 11068–11076 (2013).
[16]J.-T. Cao, X.-Y. Hao, Y.-D. Zhu, K. Sun, and J.-J. Zhu, Anal. Chem. **84**(15), 6775–6782 (2012).
[17]D. M. Lewis, H. E. Abaci, Y. Xu, and S. Gerecht, Biofabrication **7**(4), 045010 (2015).
[18]H. E. Abaci, R. Devendra, Q. Smith, S. Gerecht, and G. Drazer, Biomed. Microdevices **14**(1), 145–152 (2012).

[19]B. Srinivasan, A. R. Kolli, M. B. Esch, H. E. Abaci, M. L. Shuler, and J. J. Hickman, J. Lab. Autom. **20**(2), 107–126 (2015).
[20]J. A. Stolwijk, K. Matrougui, C. W. Renken, and M. Trebak, Pflügers Archiv-Eur. J. Physiol. **467**(10), 2193–2218 (2015).
[21]C. Ives, S. Eskin, and L. McIntire, In Vitro Cell. Dev. Biol. **22**(9), 500–507 (1986).
[22]H. Inoguchi, T. Tanaka, Y. Maehara, and T. Matsuda, Biomaterials **28**(3), 486–495 (2007).
[23]A. Ishibazawa, T. Nagaoka, T. Takahashi, K. Yamamoto, A. Kamiya, J. Ando, and A. Yoshida, Invest. Ophthalmol. Visual Sci. **52**(11), 8496–8504 (2011).
[24]X. Gao, P. Kouklis, N. Xu, R. D. Minshall, R. Sandoval, S. M. Vogel, and a. B. Malik, Am. J. Phys.: Lung Cell. Mol. Physiol. **279**(6), L1218–L1225 (2000).